



OPEN ACCESS

EDITED BY

Xiongbo Duan,
Central South University, China

REVIEWED BY

Ruikun Wang,
North China Electric Power University,
China
Hui Liang,
Harbin Engineering University, China

*CORRESPONDENCE

Xianghui Lu,
✉ x.zheng.ty@foxmail.com

RECEIVED 12 April 2023

ACCEPTED 24 May 2023

PUBLISHED 13 June 2023

CITATION

Zheng X, Lu X, Gao Y, Jin D, Hu Y, Hu Y and Mao Y (2023), Experimental study on friction pressure drop and circumferential heat transfer characteristics in helical tubes.

Front. Energy Res. 11:1204850.
doi: 10.3389/fenrg.2023.1204850

COPYRIGHT

© 2023 Zheng, Lu, Gao, Jin, Hu, Hu and Mao. This is an open-access article distributed under the terms of the [Creative Commons Attribution License \(CC BY\)](https://creativecommons.org/licenses/by/4.0/). The use, distribution or reproduction in other forums is permitted, provided the original author(s) and the copyright owner(s) are credited and that the original publication in this journal is cited, in accordance with accepted academic practice. No use, distribution or reproduction is permitted which does not comply with these terms.

Experimental study on friction pressure drop and circumferential heat transfer characteristics in helical tubes

Xiong Zheng, Xianghui Lu*, Yaxin Gao, Desheng Jin, Yisong Hu, Yousen Hu and Yulong Mao

China Nuclear Power Technology Research Institute Co., Ltd., Shenzhen, China

Helical tubes are widely used in nuclear plants, heat recovery process, and refrigeration technology. The fluid is influenced by centrifugal force flow through the helical tube, accompanied by secondary flow which is conducive to the enhancement of heat transfer. However, the uneven circumferential heat transfer caused by the secondary flow was seldom reported, while the pressure drops and heat transfer characteristics of helical tubes under single-phase and two-phase flow conditions need to be supplemented. This paper investigated the friction pressure drop and circumferential heat transfer characteristics based on the experiments on helical tubes with the coil diameter to the tube diameter varying from 28.5 to 128.5 and lift angle varying from 3° to 10°. The results showed that the coil diameter was the key parameter affecting the pressure drop and non-uniform circumferential heat transfer, compared with the lift angle. At the same cross section, the heat transfer coefficient at the outside tube wall was the highest, which was more obvious under small coil diameter conditions. Correlations of flow resistance and heat transfer were proposed for the single-phase and saturated boiling two-phase flow, respectively, and the predicted values were improved compared with the prediction results of correlations in the existing literature.

KEYWORDS

helical tube, circumferential distribution, heat transfer, pressure drop, two-phase flow

1 Introduction

Helical tubes have been widely used in nuclear plants, heat recovery process, and refrigeration technology, by virtue of compact structure, high heat transfer efficiency, and free thermal expansion (Vashisth et al., 2008; Chung et al., 2013; Fsadni and Whitty, 2016). Affected by gravity and the centrifugal force, the fluid in helical tubes flows along the axial direction accompanied by local secondary flow. The secondary flow is helpful in enhancing the internal fluid blend and strengthening the heat transfer, which is one of the important reasons why the heat transfer efficiency in the helical tube is higher than that in the straight tube (Naphon and Wongwiset, 2006). The secondary flow associated with the main flow direction in the helical tube makes the fluid flow and heat transfer process more complicated. Scholars have carried out studies on the flow resistance and heat transfer process in the helical tubes with different structural parameters and operating parameters.

Kong et al. (2017) studied the heat transfer in the helical tube with the diameter ratio (coil diameter to tube diameter, Di/d) varying from 27.5 to 47.5 and found that the heat

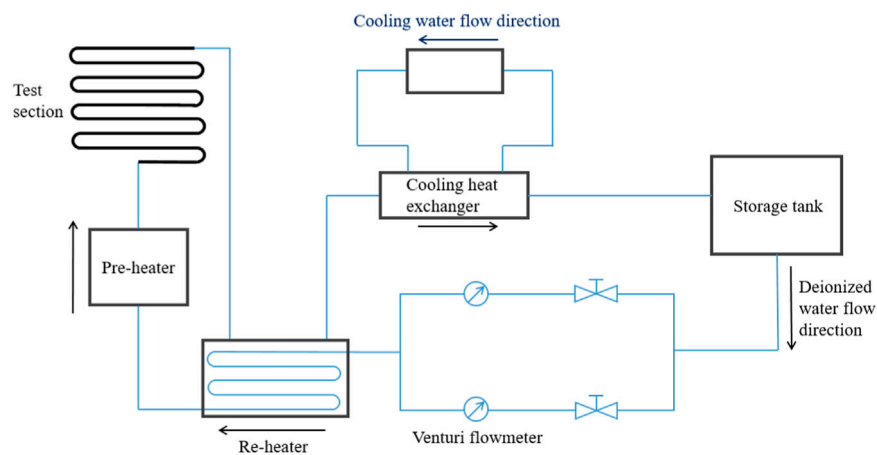


FIGURE 1
Schematic diagram of the experimental apparatus.

transfer coefficient of subcooled boiling increased with the increase in pressure and decreased with the increase in inlet subcooling degree. [Hardik et al. \(2015\)](#) studied the local heat transfer characteristics of helical tubes whose diameter ratio varied from 13.1 to 67 and proposed correlations for the inner, outer, and overall average Nu of helical tubes under single-phase conditions. [Chen et al. \(2018\)](#) conducted an experimental study on the subcooled boiling heat transfer characteristics of helical tubes with a diameter ratio of 22.4–26.2, using water as the medium. The results showed that heat flux and system pressure had significant effects on the subcooled boiling heat transfer process, and heat transfer correlations were proposed. [Nariai et al. \(1982\)](#) studied the two-phase heat transfer characteristics of helical tubes heated by liquid sodium and found that the effect of the coiled tube on the average heat transfer coefficients was small. [Seban and McLaughlin \(1963\)](#) conducted experimental studies on helical tubes with a diameter ratio of 17–104 and obtained the flow resistance characteristics of oil in laminar flow and the heat transfer characteristics of water in turbulent flow. The results showed that the coil diameter had a significant impact on the heat transfer process in turbulent flow.

In general, current research studies on the flow and heat transfer characteristics of the helical tube focuses on the thermal parameters such as mass flow rate and pressure, as well as the structural parameters such as coil diameter and tube diameter. Flow resistance and heat transfer correlations were proposed based on the experimental results. However, there are few literature works to study the flow resistance and heat transfer characteristics under single-phase and two-phase conditions on the same experimental apparatus, and the non-uniform circumferential heat transfer, which was caused by the secondary flow, was seldom analyzed.

This paper conducted experiments under single-phase and two-phase conditions based on a helical tube flow resistance and heat transfer apparatus. The effects of coil diameter and lift angle on the circumferential non-uniformity heat transfer and friction pressure drop were analyzed.

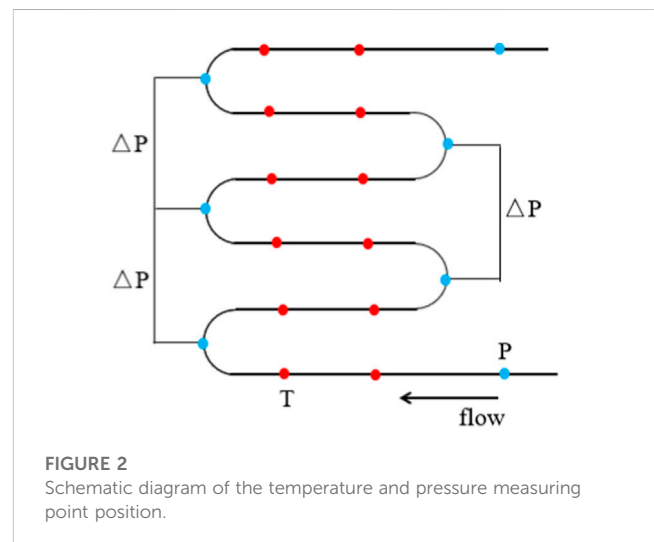


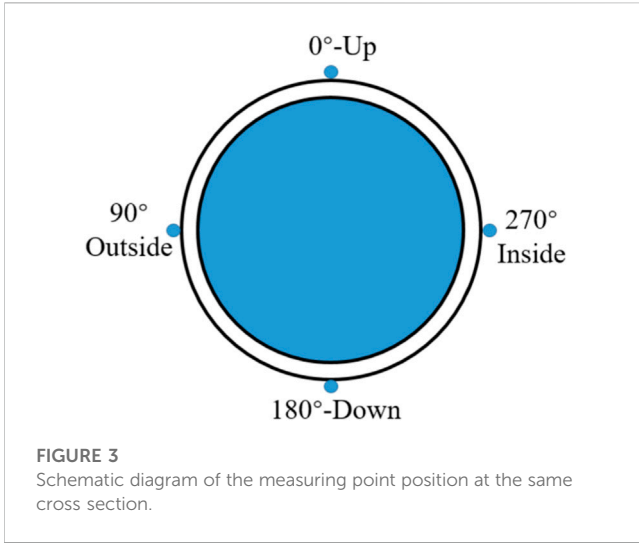
FIGURE 2
Schematic diagram of the temperature and pressure measuring point position.

2 Methodology

2.1 Helical tube thermal hydraulic apparatus

[Figure 1](#) shows the schematic diagram of the experiment system and the physical diagram of the studied helical tube test section, while [Figure 2](#) shows the position of temperature and pressure measuring point. The experiment system consists of the circulatory system and the measuring system. The deionized water from the water storage tank is first measured using the Venturi flowmeter and then heated to preset temperature using the reheater and preheater. After being heated in the test section, the backwater returns to the storage tank through the reheater and cooling heat exchanger.

Flow rate, pressure, and temperature were the three main parameters needed to be measured. The measuring accuracy of the Venturi flowmeter was 0.5. The pressure was measured using the differential pressure transmitter arranged along the helical tubes. Moreover, multiple armored N-type thermocouples were



introduced to measure temperature at four different directions on the same measuring cross section, as shown in Figure 3.

Parameters of helical tubes employed in the experiment are shown in Table 1. All helical tubes were made of S30408 stainless steel. The single-phase and two-phase experiments were carried out on each tube under different mass flow rates, heat flux, and pressure. The range of test condition was as follows: mass flow rate 100–1200 kg/(m²·s), pressure 2–7.6 MPa, and heat flux 100–500 kW/m².

2.2 Analysis methods

2.2.1 Typical reaction case analysis

The pressure drop of the steady flow in the helical tube consists of three parts: friction pressure drop, gravity pressure drop, and acceleration pressure drop:

$$\Delta P = \Delta P_f + \Delta P_g + \Delta P_a \tag{1}$$

Under the single-phase condition, the gravity pressure drop and acceleration pressure drop can be calculated as follows:

$$\Delta P_g = \int_{L_i}^{L_j} \rho_l g \sin \theta dz, \tag{2}$$

$$\Delta P_a = \left(\frac{1}{\rho_j} - \frac{1}{\rho_i} \right) G^2 = (\nu_j - \nu_i) G^2, \tag{3}$$

where ρ_i is the density of i, kg/m³; and G is the mass flow density, kg/(m²·s).

The single-phase friction pressure drop coefficient can be calculated as follows:

$$\Delta P_f = \Delta P - \Delta P_g - \Delta P_a = f_c \frac{L_{ij}}{d} \frac{\rho v^2}{2} = f_c \frac{2L_{ij}G^2}{d\rho_{ij}}, \tag{4}$$

where L_{ij} is the distance between i and j; and f_c is the friction pressure drop coefficient.

Under the two-phase condition, based on the assumption of the homogeneous flow model, the gravity pressure drop and acceleration pressure drop can be calculated as follows:

$$\Delta P_g = \int_{L_i}^{L_j} \rho_m g \sin \theta dz = g \sin \theta \int_{L_i}^{L_j} \frac{1}{\nu_f + (\nu_g - \nu_f)x(z)} dz, \tag{5}$$

$$\begin{aligned} \Delta P_a &= G^2 [\nu_f + (\nu_g - \nu_f)x_j - \nu_f - (\nu_g - \nu_f)x_i] \\ &= (\nu_g - \nu_f)(x_j - x_i)G^2, \end{aligned} \tag{6}$$

where x is the void fraction.

The friction pressure drop of the two-phase flow could be expressed with a two-phase multiplier (Lockhart and Martinelli, 1949) based on the single-phase friction pressure drop coefficient:

$$\left(\frac{dp}{dz} \right)_{tp} = \phi_{lo}^2 \left(\frac{dp}{dz} \right)_{sp}, \tag{7}$$

where $\left(\frac{dp}{dz} \right)_{tp}$ is the two-phase friction pressure drop; $\left(\frac{dp}{dz} \right)_{sp}$ is the liquid-phase friction pressure drop; and ϕ_{lo}^2 is the two-phase multiplier, $\phi_{lo}^2 = \frac{\rho_l}{\rho_m} \frac{f_{tp}}{f_l}$.

2.2.2 Wall temperature and heat transfer coefficient

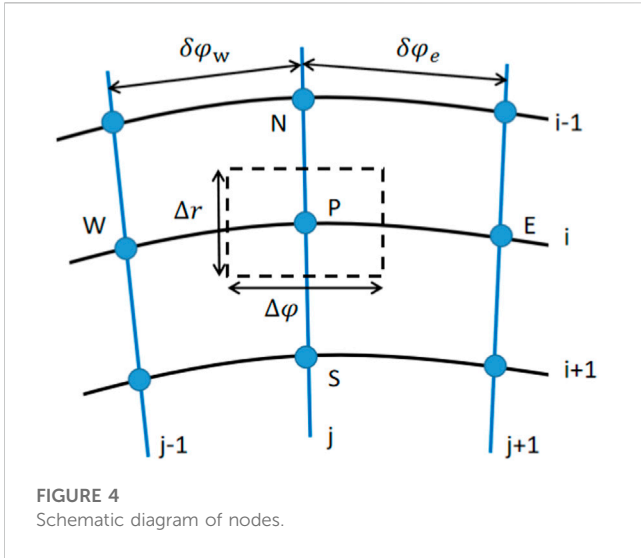
The calculation of wall temperature and heat transfer coefficient was processed on the following assumptions:

- Ignore the axial heat conduction process.
- The outside tube wall is insulated, and the whole heat conduction process is in the steady state.
- The radial thermal conductivity stays constant.

Based on the aforementioned assumptions, the heat conduction process from the outside wall to the inside wall can be regarded as a two-dimensional steady heat conduction process. The heat conduction equation in polar coordinates is

TABLE 1 Structural parameters of helical tubes.

Serial number	Tube diameter (mm)	Coil diameter (mm)	Length (mm)	Lift angle (°)	
1		14	400	8,200	5
2		14	735	8,100	5
3		14	1,050	10,700	5
4		14	1800	14,200	5
5		14	1,050	8,200	3
6		14	1,050	8,360	10



$$\frac{1}{r} \frac{\partial}{\partial r} \left(r \lambda \frac{\partial T}{\partial r} \right) + \frac{1}{r} \frac{\partial}{\partial \varphi} \left(\frac{\lambda}{r} \frac{\partial T}{\partial \varphi} \right) + \dot{\phi} = 0. \quad (8)$$

The helical tube wall was divided into $N_i \times N_j$ blocks, and Eq. 8 was dispersed on the control body, as shown in Figure 4:

$$a_P T(i, j) = a_E T(i, j + 1) + a_W T(i, j - 1) + a_S T(i + 1, j) + a_N T(i - 1, j) + S, \quad (9)$$

where

$$a_N = \frac{\Delta \varphi r_N \lambda_N}{\delta r_N}, a_S = \frac{\Delta \varphi r_s \lambda_s}{\delta r_s}, a_E = \frac{\Delta r \lambda_E}{r_E \delta \varphi_E}, a_W = \frac{\Delta r \lambda_W}{r_W \delta \varphi_W},$$

$$a_P = a_W + a_E + a_S + a_N, S = \frac{\Delta r \Delta \varphi (r_N + r_s) \Phi}{2}, \Phi = \frac{P \eta}{\pi (R^2 - r^2) L_h}.$$

The inside wall temperature of the tubes could be obtained by using the space node progression algorithm based on the measured outside wall temperature.

The resistivity of 304 stainless steel has a linear relationship with temperature in the experimental temperature range (Taler and Zima, 1999), which had been considered in the calculation of heat flux:

$$q_i = \frac{P \eta}{A_s} = \frac{I^2 \eta}{\pi d L_h} \cdot \rho(T) \frac{L_h}{S} = \frac{I^2 \eta}{\pi d S} \rho(T), \quad (10)$$

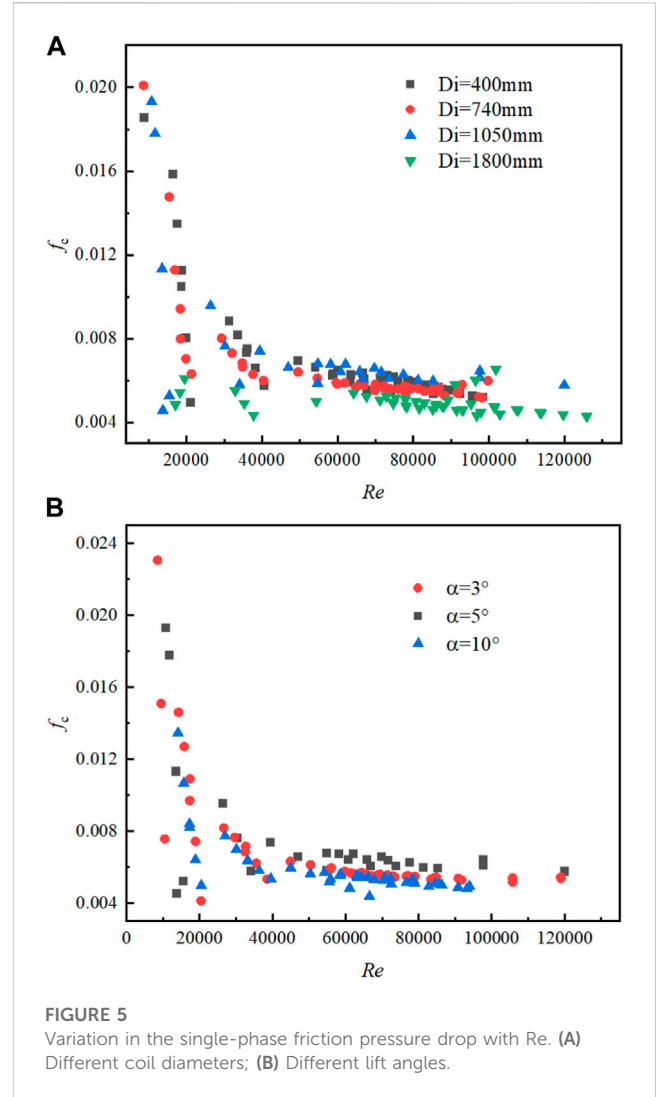
where q_i is the heat flux at point i , W/m^2 ; P is the heat power, W ; I is the electricity, A ; and η is the heating efficiency, which was obtained with the single-phase experiment before.

The average main flow enthalpy at the measurement point i can be calculated as follows:

$$H_i = H_{i-1} + \frac{q_i \pi d (L_i - L_{i-1})}{M}, \quad (11)$$

where H_i is the enthalpy at point i , kJ/kg ; and M is the mass flow rate, kg/s .

The main flow temperature at point i could be obtained from water property with pressure and enthalpy. Hence, the heat transfer coefficient can be calculated as



$$h_i = \frac{q_i}{T_{wi} - T_{fi}}, \quad (12)$$

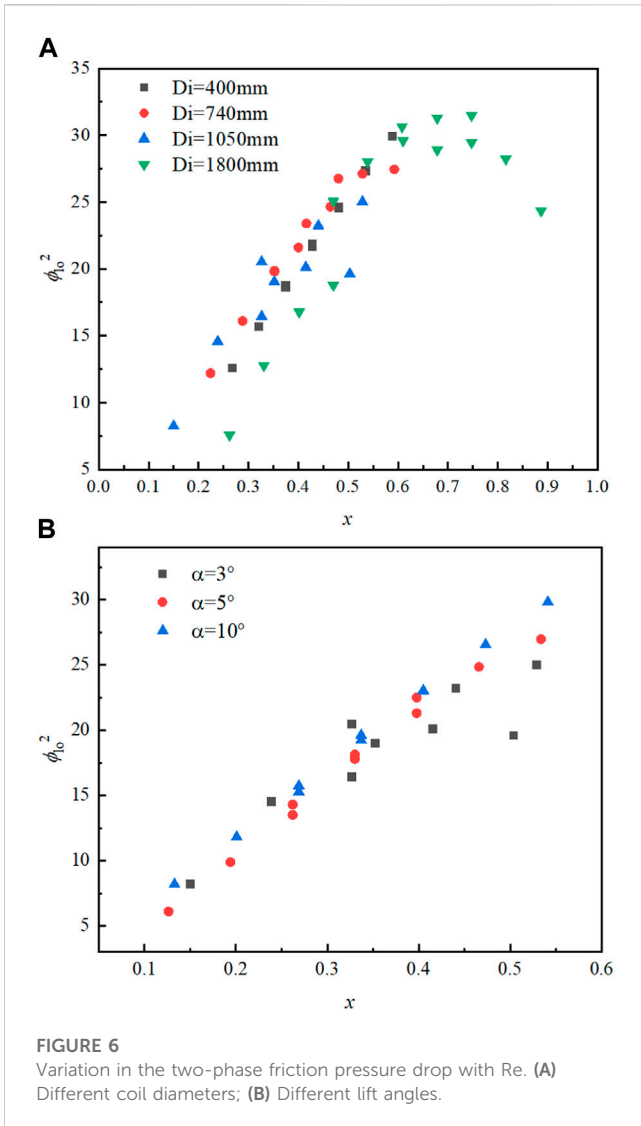
where h_i is the heat transfer coefficient at point i , $W/(m^2 \cdot ^\circ C)$; T_{wi} is the wall temperature inside the tube, $^\circ C$; and T_{fi} is the main flow temperature, $^\circ C$.

The heat transfer coefficient of each point on the same cross section (as shown in Figure 3) was switched to dimensionless h for the evaluation of circumferential heat transfer intensity:

$$h^* = \frac{h_i}{h_{ave}}, \quad (13)$$

where h_{ave} is the average temperature of the cross section, which is calculated with the temperature at four section inner wall temperature.

It is worth mentioning that h_{ave} is not equal to the average of h_i at the four directions, and h^* could reflect the relative value of the heat transfer coefficient of each side, to evaluate the heat transfer intensity.



3 Results and discussion

3.1 Friction pressure drop

Figure 5A shows the variation in the single-phase friction pressure drop with Re with different coil diameters. The friction coefficient of each tube is approximately negatively exponential with Re at $D_i < 1800$ mm, while the fc changes smoothly with Re at $D_i = 1800$ mm. Moreover, the fc at $D_i = 1800$ mm is smaller than that in other tubes at the same Re. This might be explained that helical tubes with large coil diameter has a similar flow pattern to the straight tubes, meaning that there is less secondary flow in large coil diameter tubes and smaller energy dissipation.

Figure 5B shows the variation in the single-phase friction pressure drop with Re at different lift angles. The friction coefficient of each tube is approximately negatively exponential with Re under the same coil diameter D_i , which indicates that the lift angle has no significant effect on the friction pressure drop coefficient.

Figures 6A, B show the variation in the two-phase multiplier with void fraction x at different coil diameters and different lift angles, respectively, when $p = 3.75$ MPa and $G = 405$ kg/(m³·s). It could be seen that the two-phase multiplier shows a similar trend with the variation in the void fraction. A peak value of the two-phase multiplier appears at $x = 0.75$ when $D_i = 1800$ mm, and a similar trend was reported by Santini et al. (2008).

3.2 Single-phase circumferential non-uniformity characteristics

Figure 7 shows the variation in h^* with a void fraction at different coil diameters when $p = 3.75$ MPa and $G = 920$ kg/(m³·s), and the heat transfer coefficient of the straight tube predicted by the Dittus–Boelter (D–B) equation (Heiss and Coull, 1951) is also provided. It can be seen that h^* predicted by the D–B equation is smaller than 1.0, which confirms that the average heat transfer of the helical tube is stronger than that of the straight tube. Moreover, as the figure shows, the outside h^* at the same cross section is the largest, while the up and down sides h^* have similar values. The inside h^* is the smallest and always less than the predicted value of the D–B equation. The outside h^* decreases gradually with an increase in the coil diameter. When $D_i = 400$ mm, the outside h^* is more than 2.0, and the maximum h^* is 2.58. When $D_i = 1800$ mm, the outside h^* decreases to less than 1.5, and the maximum h^* is 1.35, which is 1.23 lower than that in the $D_i = 400$ mm tube.

It might be explained from two points. One is that the cold fluid with higher density, affected by gravity and centrifugal force, tends to gather in the outside wall where the temperature difference between the outside fluid and wall is larger. The other is that the flow rate of the outside fluid is higher than that of the inside fluid, which benefits to improve the convection heat transfer. The smaller the coil diameter is, the stronger the centrifugal force effect on the fluid, meaning that the fluids with different temperatures and densities would be separated more completely. Hence, the phenomenon of larger outside h^* at the same cross section is more obvious in the tubes with small coil diameter.

Figure 8 shows the variation in h^* with a void fraction under different lift angle conditions when $p = 3.75$ MPa and $G = 920$ kg/(m³·s). It can be seen that the outside h^* is the largest, and the inside h^* is the smallest at different lift angles. Additionally, the maximum h^* on the outside is 1.71 at $\alpha = 3^\circ$, which is only 0.17 higher than the maximum at $\alpha = 10^\circ$. The lift angle has no significant effect on the outside h^* . It might be explained that the lift angle has slight influence on the distribution of fluid with different temperatures and densities, and the heat transfer coefficient in different directions was mainly affected by the coil diameter.

3.3 Two-phase circumferential non-uniformity characteristics

Figure 9 shows the variation in h^* with a void fraction under different coil diameter conditions when $p = 3.75$ MPa and $G = 405$ kg/(m³·s), and the heat transfer coefficient of the straight tube

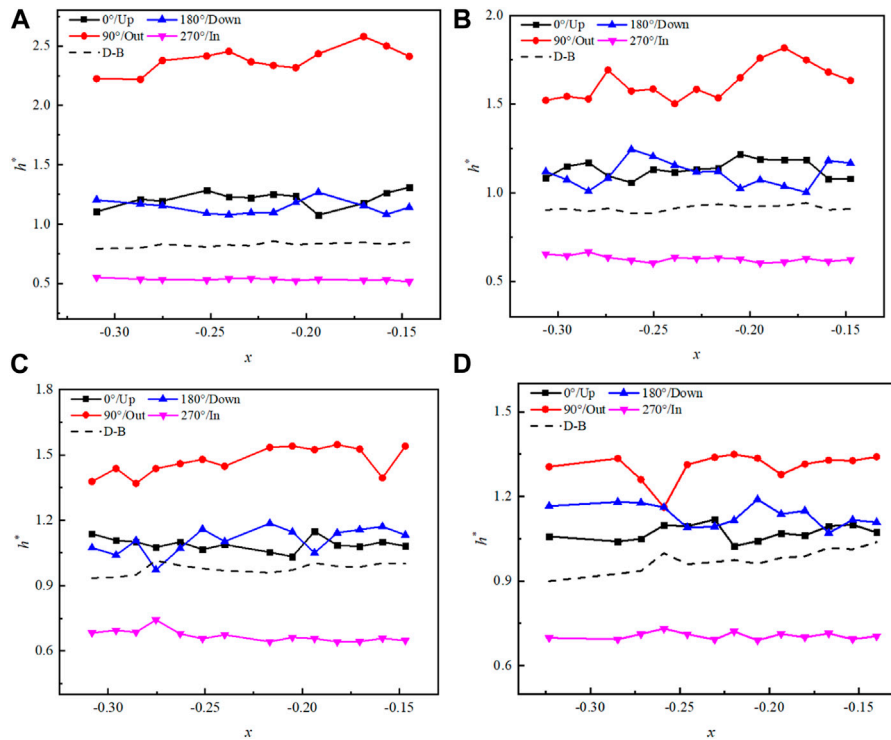


FIGURE 7 Variation in h^* with a void fraction when $p = 3.75$ MPa and $G = 920$ kg/(m³·s). (A) $D_i = 400$ mm; (B) $D_i = 735$ mm; (C) $D_i = 1050$ mm; and (D) $D_i = 1800$ mm.

predicted by the Chen equation (Chen, 1962) is also provided. It can be seen that as the coil diameter increase from 400 to 1800 mm, the outside h^* maintain the highest compared with h^* in other three directions at the same cross section. This phenomenon is more significant at $D_i = 400$ mm, and h^* even exceeds 4.0 at $x = 0.44$, meaning that the outside h is four times the average h . Additionally, h^* in each direction is higher than that predicted by the Chen correlation, except when $x > 0.2$ at $D_i = 400$ mm.

It might be explained that the density difference between the gas phase and liquid phase is larger than that in different liquid temperatures, and the gas tends to separate much completely from liquid under the same centrifugal force and gravity. Hence, the dense liquid gravitates to gather outside, and the bubble gravitates to gather inside, which leads to the significant difference of outside h^* and inside h^* . This phenomenon is weakened with the increase in the coil diameter contributing to the decrease in centrifugal force. The outside h^* decreases to less than 1.4 when $D_i = 1800$ mm.

Figure 10 shows the variation in h^* with a void fraction under different lift angle conditions when $p = 3.75$ MPa and $G = 405$ kg/(m³·s). It can be seen that the lift angle shows no obvious regular influence on the distribution of h^* . The similar opinion about the lift angle was proposed under single-phase conditions, further indicating that the lift angle is not the vital structural parameter affecting the temperature and heat transfer distribution in the helical tube.

3.4 Correlations between the friction pressure drop and heat transfer

3.4.1 Friction pressure drop

Figure 11 shows the experimental single-phase friction pressure drop coefficient and the values predicted by the empirical correlations. It can be seen that f_{c-cal} predicted by Ito (1959) and Srinivasan et al. (1968) all underestimates the experiment value when $f_{c-exp} > 0.01$, and there is still a maximum error of 81% (at $f_{c-exp} = 0.004$, Srinivasan). The Blasius correlation was proposed with straight tube experiments, in which the predicted value is all smaller than the experimental value. The Ito and Srinivasan correlations were proposed with helical tube experiment, and different structural parameters and operating parameters might be the dominating factors contributing to errors.

Based on the single-phase experimental pressure data, the correction of f_c is shown in Eq. 14:

$$f_c = \frac{0.0791}{Re^{0.25}} + \frac{81858}{Re^{1.54}} \left(\frac{d}{D_c} \right)^{0.48}, \quad (14)$$

$$D_c = D_i (1 + \tan \alpha).$$

Figure 12 shows the experimental two-phase friction pressure drop coefficient and the values predicted by the empirical correlations. It can be seen that Hardik and Prabhu (2017) and Xiao et al. (2018)

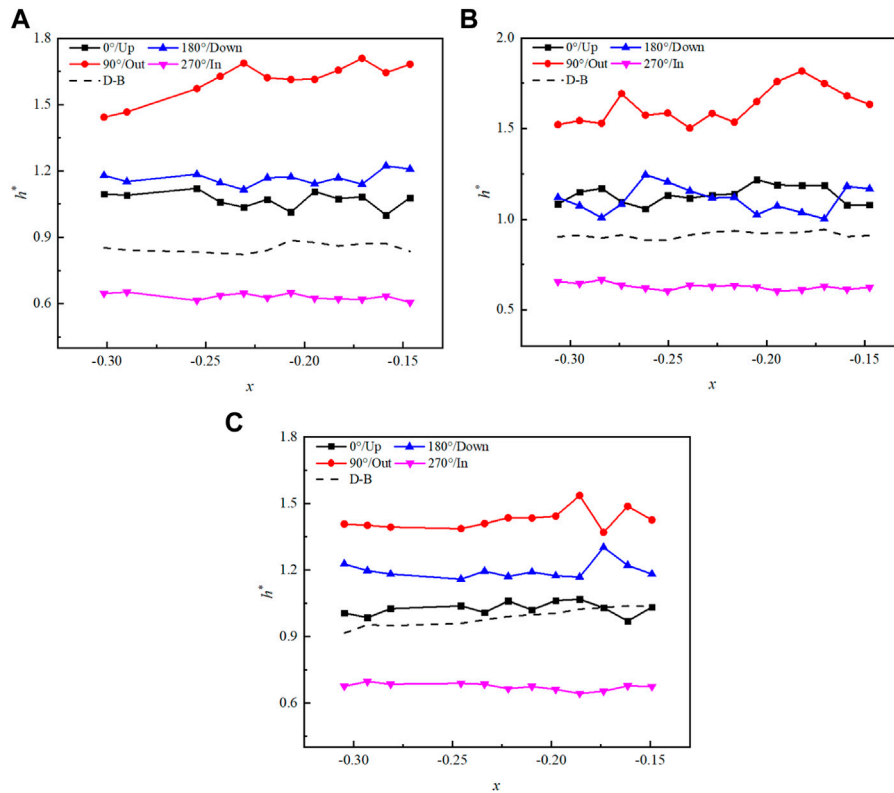


FIGURE 8 Variation in h^* with a void fraction when $p = 3.75$ MPa and $G = 920$ kg/(m³·s). (A) $\alpha = 3^\circ$; (B) $\alpha = 5^\circ$; and (C) $\alpha = 10^\circ$.

overestimated the pressure drop, while Ju et al. (2001) underestimated the pressure drop. Ju et al. found that the two-phase multiplier might be revised by the polynomial related to the void fraction:

$$\begin{aligned} \phi_{lo}^2 &= f(x) \left[1 + x \left(\frac{\rho_f}{\rho_g} - 1 \right) \right] \left[1 + x \left(\frac{\mu_g}{\mu_f} - 1 \right) \right]^{0.25}, \\ \phi_{lo}^2 &= (1.23 + 4.47x - 9.28x^2 + 3.2x^3) \\ &\times \left[1 + x \left(\frac{\rho_f}{\rho_g} - 1 \right) \right] \left[1 + x \left(\frac{\mu_g}{\mu_f} - 1 \right) \right]^{0.25}, \end{aligned} \quad (15)$$

The mean error (ME), mean absolute error (MAE), and root mean square error (RMSE) were employed to evaluate the predicted value, which are calculated as follows:

$$ME = \sum \frac{f_{c-cal} - f_{c-exp}}{f_{c-exp}} \times 100\%, \quad (16)$$

$$MAE = \sum \frac{|f_{c-cal} - f_{c-exp}|}{f_{c-exp}} \times 100\%, \quad (17)$$

$$RMSE = \sqrt{\frac{\sum (f_{c-cal} - f_{c-exp})^2}{N}}, \quad (18)$$

The comparison between the predicted value and the experimental value is given in Table 2 and Table 3, respectively. It can be seen that the value calculated using Eq. 14 and Eq. 15 is more consistent with the experimental value, and the MAE and RMSE are smaller than the predicted value in the literature.

3.4.2 Heat transfer

Based on the classical D-B equation for a straight tube, considering the influence of the coil diameter and lift angle, the average heat transfer coefficient at the single phase could be fitted as follows:

$$Nu_{ave} = 0.052 Re^{0.77} Pr^{0.4} \left(\frac{d}{D_c} \right)^{0.092}, \quad (20)$$

However, according to the discussion on the circumferential non-uniformity of the aforementioned helical tubes, the heat transfer coefficient in different directions at the same cross section could be very different, and the outside h in small coil diameter tubes could reach 3–4 times the average heat transfer coefficient. Hence, only Eq. 20 cannot reflect the vital circumferential non-uniformity of the heat transfer in helical tubes. The factor λ was proposed to evaluate the circumferential heat transfer intensity, and it was considered to be the function of Re and diameter ratio D_i/d :

$$\lambda_i = \frac{Nu_i}{Nu_{ave}} = f \left(Re, \frac{d}{D} \right), \quad (21)$$

Table 4 shows the deviation between the experimental value and the predicted value under single-phase conditions. It can be seen that the max MAE was 13.73%, while the max RMSE was 49.63.

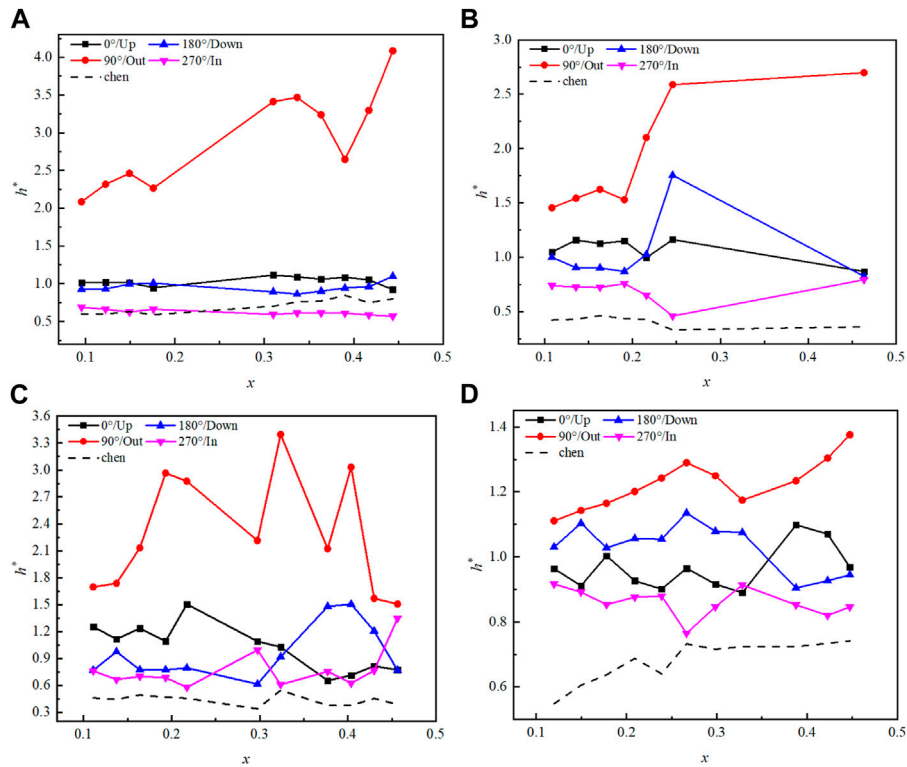


FIGURE 9 Variation in h^* with a void fraction when $p = 3.75$ MPa and $G = 920$ kg/(m²·s). (A) $D_i = 400$ mm; (B) $D_i = 735$ mm; (C) $D_i = 1050$ mm; and (D) $D_i = 1800$ mm.

The λ fitted with experimental results in different directions is given as follows:

$$\lambda_{up} = 0.187Re^{0.195} \left(\frac{d}{D_c}\right)^{0.094}, \quad (22)$$

$$\lambda_{out} = 1.789Re^{0.114} \left(\frac{d}{D_c}\right)^{0.316}, \quad (23)$$

$$\lambda_{down} = 4.751Re^{-0.138} \left(\frac{d}{D_c}\right)^{-0.023}, \quad (24)$$

$$\lambda_{in} = 2.06Re^{-0.159} \left(\frac{d}{D_c}\right)^{-0.142}, \quad (25)$$

The modified Chen correlation considers that the saturated boiling heat transfer h in helical tubes could be divided into forced convection part h_c and nucleate boiling part h_{NB} :

$$h = h_c + h_{NB}, \quad (25a)$$

Referring to the modified Chen correlation and the D-B equation, the forced convection h_c is fitted as follows:

$$h_c = 0.023Re_L^{0.9} Pr^{0.4} \frac{\lambda}{d} \left(\frac{d}{D_c}\right)^{0.04} F, \quad (26)$$

where

$$F = \begin{cases} 1, & \frac{1}{X_{tt}} \leq 0.1, \\ 2.35 \left(\frac{1}{X_{tt}} + 0.213\right)^{0.736}, & \frac{1}{X_{tt}} > 0.1, \end{cases} \quad (27)$$

$$h_{NB} = 0.0215 \frac{\lambda^{0.79} c_{pf}^{0.45} \rho_f^{0.49}}{\sigma^{0.5} \mu_f^{0.29} h_{fg}^{0.24} \rho_g^{0.24}} \Delta T_{sat}^{0.24} \Delta P_{sat}^{0.75} S$$

where

$$S = \begin{cases} [1 + 0.12 (Re_{TP}^*)^{1.14}]^{-1}, & Re_{TP}^* < 32.5 \\ [1 + 0.42 (Re_{TP}^*)^{0.78}]^{-1}, & 32.5 \leq Re_{TP}^* < 70 \\ 0.1, & Re_{TP}^* \geq 70 \end{cases}$$

$$Re_L = \frac{G(1-x)D_i}{m_f}, X_{tt} = \left(\frac{1-x}{x}\right)^{0.9} \left(\frac{\rho_g}{\rho_f}\right)^{0.5} \left(\frac{\mu_f}{\mu_g}\right)^{0.1},$$

$$Re_{TP}^* = Re_L F^{1.25} \times 10^{-4}$$

Table 5 shows the deviation between the experimental value and predicted value under two-phase conditions. It can be seen that compared with the modified Chen correlation, the value predicted by the correlation proposed by this paper is more consistent with the

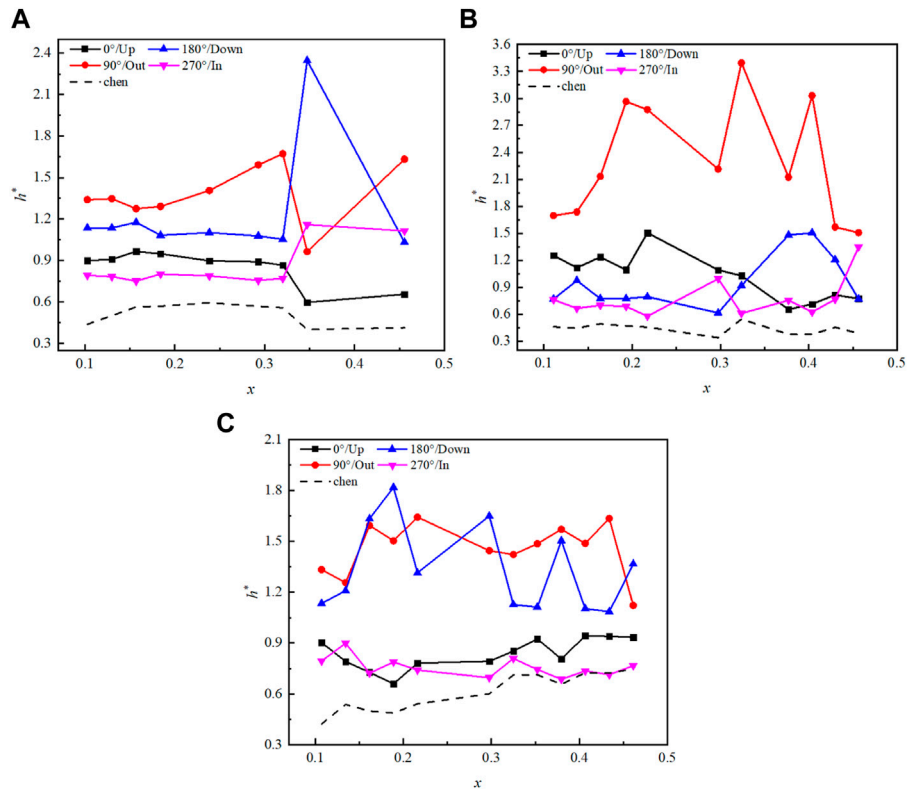


FIGURE 10 Variation in h^* with the void fraction when $p = 3.75$ MPa and $G = 920$ kg/(m³·s). (A) $\alpha = 3^\circ$; (B) $\alpha = 5^\circ$; and (C) $\alpha = 10^\circ$.

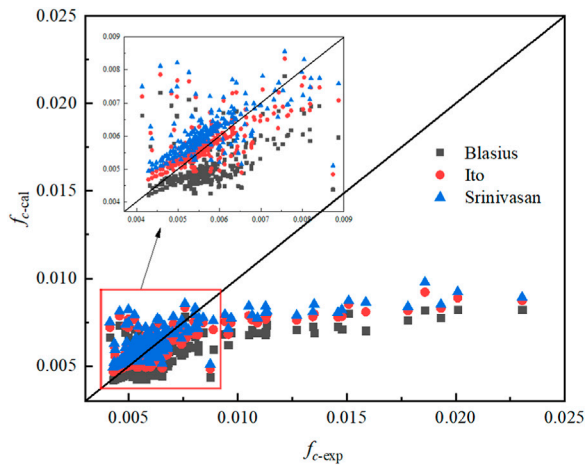


FIGURE 11 Comparison of the experimental value and the predicted value under single-phase conditions.

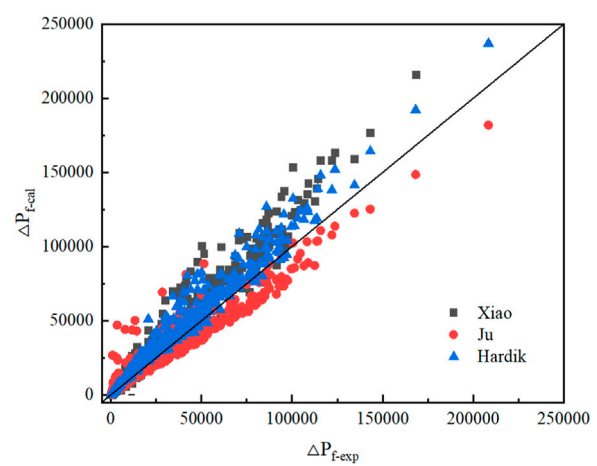


FIGURE 12 Comparison of the experimental value and the predicted value under two-phase conditions.

experimental value, of which the ME, MAE, and RMSE are greatly improved.

The correlations proposed in this paper have an applicable parameter range of $D_i/d = 28.6\text{--}128.6$, $G = 200\text{--}1,000$ kg/(m²·s), and $P = 2\text{--}7.6$ MPa.

4 Conclusion

In order to study the flow resistance and the non-uniform characteristics of circumferential heat transfer in helical tubes, the experiments of helical tubes with different coil diameters and

TABLE 2 Error between the experimental value and predicated value under single-phase conditions.

Reference	ME (%)	MAE (%)	RMSE
Blasius	-13.73	16.71	0.00232
Ito	-1.61	9.85	0.00204
Srinivasan	4.21	12.51	0.00199
Eq. 14	-1.34	12.26	0.00139

TABLE 3 Error between the experimental value and predicated value under two-phase conditions.

Reference	ME (%)	MAE (%)	RMSE
Xiao	35.48	38.85	13,644.01
Ju	31.34	51.85	9,770.83
Hardik	29.94	30.80	10,333.87
Eq. 15	13.56	30.79	6,714.45

TABLE 4 Error between the experimental value and predicated value of Nu in different directions.

Correlation	ME (%)	MAE (%)	RMSE
Nu_{ave}	2.26	7.13	14.22
$\lambda_{up} Nu_{ave}$	3.53	11.94	21.93
$\lambda_{out} Nu_{ave}$	2.86	13.73	49.63
$\lambda_{down} Nu_{ave}$	2.90	9.86	22.37
$\lambda_{in} Nu_{ave}$	3.14	6.01	7.02

TABLE 5 Error between the experimental value and predicated value of Nu under two-phase conditions.

Correlation	ME (%)	MAE (%)	RMSE
Modified Chen	-97.58	97.58	95,997.63
Eq. 25	16.96	30.85	34,843.62

lift angles were carried out under single-phase conditions and saturated boiling two-phase conditions. The friction pressure drop and circumferential heat transfer coefficient were analyzed, and the empirical correlations of heat transfer and flow resistance were obtained based on the experimental results. The following conclusions were obtained:

- (1) Increasing coil diameter is conducive to reducing the flow resistance, while the lift angle has no significant effect on the friction pressure drop.

- (2) The outside heat transfer coefficient is the maximum at the same cross section, and the inside heat transfer coefficient is the minimum, which is more obvious under two-phase conditions or in the tubes with a small coil diameter.
- (3) The lift angle has no obvious effect on circumferential heat transfer non-uniformity.
- (4) λ was proposed to present the circumferential non-uniformity in helical tubes, which was fitted with the single-phase experimental results.
- (5) Based on the experimental results of single-phase conditions and two-phase conditions, the flow resistance correlation and the heat transfer correlation are fitted, respectively.

Data availability statement

The original contributions presented in the study are included in the article/Supplementary Material; further inquiries can be directed to the corresponding author.

Author contributions

XL and YoH contributed to the conception. YM and YiH contributed to methodology. YG and XZ organized the database and performed the statistical analysis. XZ wrote the first draft of the manuscript. DJ and XZ wrote sections of the manuscript. All authors contributed to the article and approved the submitted version.

Funding

This research was funded by the National Natural Science Foundation of China (grant numbers U20B0211 and 52171085) and Department of Science and Technology of Guangdong Province (grant number 2017B020242001).

Conflict of interest

Authors XZ, XL, YG, DJ, YiH, YoH, and YM were employed by the company China Nuclear Power Technology Research Institute Co., Ltd.

Publisher's note

All claims expressed in this article are solely those of the authors and do not necessarily represent those of their affiliated organizations, or those of the publisher, the editors, and the reviewers. Any product that may be evaluated in this article, or claim that may be made by its manufacturer, is not guaranteed or endorsed by the publisher.

References

- Chen, J. C. (1962). Correlation for boiling heat transfer to saturated fluids in convective flow. *Ind. Eng. Chem. Process Des. Dev.* 5, 322–329. doi:10.1021/i260019a023
- Chen, S., Hu, Z., Xiao, Y., and Gu, H. (2018). Experimental investigation of subcooled flow boiling heat transfer in helical coils. *Nucl. Eng. Des.* 327, 187–197. doi:10.1016/j.nucengdes.2017.12.014
- Chung, Y.-J., Kim, H. J., Chung, B.-D., Lee, W. J., and Kim, M.-H. (2013). Thermo-hydraulic characteristics of the helically coiled tube and the condensate heat exchanger for SMART. *Ann. Nucl. Energy* 55, 49–54. doi:10.1016/j.anucene.2012.11.026
- Fsadni, A. M., and Whitty, J. P. M. (2016). A review on the two-phase heat transfer characteristics in helically coiled tube heat exchangers. *Int. J. Heat Mass Transf.* 95, 551–565. doi:10.1016/j.ijheatmasstransfer.2015.12.034
- Hardik, B. K., Baburajan, P. K., and Prabhu, S. V. (2015). Local heat transfer coefficient in helical coils with single phase flow. *Int. J. Heat Mass Transf.* 89, 522–538. doi:10.1016/j.ijheatmasstransfer.2015.05.069
- Hardik, B. K., and Prabhu, S. V. (2017). Boiling pressure drop and local heat transfer distribution of helical coils with water at low pressure. *Int. J. Therm. Sci.* 114, 44–63. doi:10.1016/j.ijthermalsci.2016.12.004
- Heiss, J. F., and Coull, J. (1951). Nomograph of dittus-boelter equation for heating and cooling liquids. *Industrial Eng. Chem.* 43, 1226–1229. doi:10.1021/ie50497a060
- Ito, H. (1959). Friction factors for turbulent flow in curved pipes. *Trans. ASME. J. Basic Eng.* 81, 123–132. doi:10.1115/1.4008390
- Ju, H., Huang, Z., Xu, Y., Duan, B., and Yu, Y. (2001). Hydraulic performance of small bending radius helical coil-pipe. *J. Nucl. Sci. Technol.* 38, 826–831. doi:10.1080/18811248.2001.9715102
- Kong, L., Han, J., Chen, C., Xing, K., and Lei, G. (2017). An experimental study on subcooled flow boiling heat transfer characteristics of R134a in vertical helically coiled tubes. *Exp. Therm. Fluid Sci.* 82, 231–239. doi:10.1016/j.expthermflusci.2016.11.023
- Lockhart, R. W., and Martinelli, R. C. (1949). Proposed correlation of data for isothermal two-phase two-component flow in pipes. *Chem. Eng. Proc.* 45.
- Naphon, P., and Wongwises, S. (2006). A review of flow and heat transfer characteristics in curved tubes. *Renew. Sustain. Energy Rev.* 10, 463–490. doi:10.1016/j.rser.2004.09.014
- Nariai, H., Kobayashi, M., and Matsuoka, T. (1982). Friction pressure drop and heat transfer coefficient of two-phase flow in helically coiled tube once-through steam generator for integrated type marine water reactor. *J. Nucl. Sci. Technol.* 19, 936–947. doi:10.1080/18811248.1982.9734239
- Santini, L., Cioncolini, A., Lombardi, C., and Ricotti, M. (2008). Two-phase pressure drops in a helically coiled steam generator. *Int. J. Heat Mass Transf.* 51, 4926–4939. doi:10.1016/j.ijheatmasstransfer.2008.02.034
- Seban, R. A., and McLaughlin, E. F. (1963). Heat transfer in tube coils with laminar and turbulent flow. *Int. J. Heat Mass Transf.* 6, 387–395. doi:10.1016/0017-9310(63)90100-5
- Srinivasan, P. S., Nandapurkar, S. S., and Holland, F. A. (1968). Pressure drop and heat transfer in coils. *Chem. Eng.* 218, 113–119.
- Taler, J., and Zima, W. (1999). Solution of inverse heat conduction problems using control volume approach. *Int. J. Heat Mass Transf.* 42, 1123–1140. doi:10.1016/s0017-9310(98)00280-4
- Vashisth, S., Kumar, V., and Nigam, K. D. P. (2008). A review on the potential applications of curved geometries in process industry. *Industrial Eng. Chem. Res.* 47, 3291–3337. doi:10.1021/ie701760h
- Xiao, Y., Hu, Z., Chen, S., and Gu, H. (2018). Experimental study of two-phase frictional pressure drop of steam-water in helically coiled tubes with small coil diameters at high pressure. *Appl. Therm. Eng.* 132, 18–29. doi:10.1016/j.applthermaleng.2017.12.074